Characterization of Cancerous Tissue by Electrochemical Method

Salma Zahid[1*], Hicham El Boté[1] and Abdelilah Chtaini[1]

[1]*University Sultan Moulay Slimane, Faculty of Science and Technology, Department of Chemistry and Environment, Beni Mellal, Morocco*

*Corresponding author: slmzahid77@gmail.com

Received 30/12/2024; accepted 21/04/2025
https://doi.org/10.4152/pea.2027450204

Abstract

Non-muscle-invasive bladder cancer (NMIBC) presents a significant challenge in terms of diagnosis, follow-up and recurrence monitoring. Current methods for follow-up, such as cystoscopy and cytology, are invasive, time-consuming, and often associated with discomfort for patients. Hence, there is a pressing need for the development of non-invasive, cost effective and efficient techniques for NMIBC monitoring. In this study, an electrochemical simplified method for the follow-up of NMIBC is proposed, offering a promising alternative to conventional approaches. The method is based on the detection of cancerous cells using a carbon paste electrode (CPE). This electrode showed considerable activity for the detection and characterization of cancerous cells which are manifested by the appearance of two redox peaks, and also a remarkable increase in specific capacitance. The effect of the presence of iron ions in the electrolytic medium showed a very considerable difference in voltammograms. Fenton reaction was manifested by two redox peaks characteristic of the presence of cancer cells.

Keywords: BC; CPE; CB; EIS; non-invasive follow up; SWV.

Introduction•

Bladder cancer (BC) is a common malignancy in women, and is the fourth most common malignancy in men [1, 2]. It includes less aggressive tumours that usually do not spread and need long-term monitoring, as well as aggressive tumours that spread quickly and are quite lethal.

Smoking and certain work-related exposures are main well-known risk factors. There is growing evidence suggesting the influence of certain dietary habits, imbalanced microbiome, interactions between genes and external risk factors, exposure to diesel exhaust emissions, and pelvic radiotherapy [3, 4].

Even if patients with non-muscle-invasive bladder cancer (NMIBC) are treated as recommended in current guidelines, they still have a high chance of the cancer coming back or getting worse, with up to 50% patients experiencing this within 5 years. Because of this, they need to be closely monitored. However, there is not a

•The abbreviations list is in page 130.

clear plan for how often or for how long this monitoring should happen. Different guidelines and risk groups suggest diverse frequencies and durations, but these recommendations are not strongly supported by evidence.

Main tools for monitoring, cystoscopy and cytology, have their limitations. Even with advanced cystoscopy techniques, follow-up still involves invasive procedures. New urine tests might help improve monitoring, showing promise in detecting cancer recurrence or progression with high accuracy. Other developments like active surveillance or outpatient treatments could lessen the burden on patients. Using these tests could be both cost-effective and better for patients, but more research is needed to be corroborate this [5-7].

Monitoring patients with NMIBC presents an ongoing challenge for urologists, with no definitive solution yet. The frequency of monitoring depends on how likely the tumour is to come back or worsen, as well as the patient's specific circumstances. Typically, urethrocystoscopy, imaging and urine cytology are suggested, but these procedures might be overly intensive for those with intermediate risk profiles. In certain cases, urine markers might enhance monitoring, although conclusive evidence from prospective randomized studies is still awaited [7, 8].

BC ranks as the ninth most prevalent cancer globally. In 2022, over 600,000 individuals have received a BC diagnosis worldwide, leading to over 220,00 deaths from the disease. Diagnosis and treatment of BC pose significant challenges and expenses. Typically, diagnosis heavily relies on cystoscopy, an invasive and costly procedure. Fortunately, most cases are detected early, when treatment is most effective. However, approximately 25% BC are diagnosed later, at more advanced stages [9].

Recently, several research studies have proposed invasive methods for the detection of biological elements of interest, including optical, amperometry and electrochemical biosensors [10-14]. Biosensors are analytical devices that incorporate biological molecules for rapid and accurate detection of target species such as proteins, antigens, viruses, bacteria and other substances. In this work, the performance of a CPE for detection of cancer cells was examined. Reaction kinetics were monitored by CV, SWV and EIS. The effect of the presence of iron in reaction efficiency was also examined.

Materials and methods

Fig. 1 shows CPE preparation, by mixing powdered carbon graphite with paraffin oil and a few drops of methanol, which acts as a temporary dispersing agent that improves CPE homogeneity, by enabling uniform mixing of graphite powder with paraffin oil, before evaporation. The mixture was incorporated into a cylindrical cavity with a surface area of 1 cm^2. Cancer cells were extracted from BC tumours, and ground with a NaCl solution. Experiments were done using an electrochemical measuring cell equipped with Ag/AgCl, Pt and CPE, as reference, auxiliary and working electrodes, respectively. Potential flow was ensured by Orrigalys potentiostat.

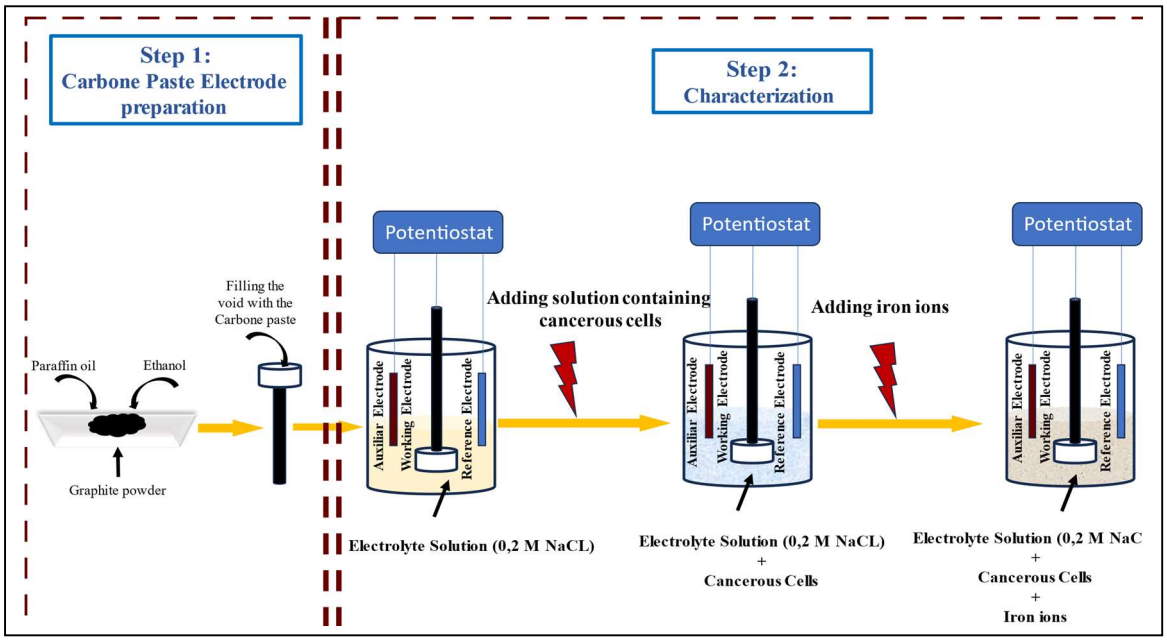

Figure 1: Steps of working protocol.

Electrochemical methods used in this work were CV, EIS, SWV and specific capacitance (Cs), which was deduced from the following formula:

$$Cs = \frac{Q}{mV} \tag{1}$$

where Cs is in F/cm^2, Q is stored charge in Columb and m is mass of the active substance in grams.

$$I = \frac{Q}{t} \qquad Q = I*t \tag{2}$$

From Eqs. (1) and (2) one finds that:

$$Cs = \frac{I}{m\,(\frac{V}{t})} \tag{3}$$

where V/t is scan rate, V_b. Hence,

$$Cs = I/\,(m\,V_b) \tag{4}$$

which implies that:

$$I = Cs*m*V_b \tag{5}$$

Current value changed when potential values changed, so that:

$$\int_{E1}^{E2} IdE \tag{6}$$

Voltammogram area is:

$$A = \int_{E1}^{E2} Cs * m * Vb\ dE \tag{7}$$

where $Cs*m*V_b$ is a constant.

$$A_1 = (E_2\text{-}E_1)\ Cs*m*V_b \text{ et } A_2 = (E_2\text{-}E_1)\ Cs*m*V_b \quad (8)$$

$$A = A_1\text{-}A_2 = 2\ (E_2\text{-}E_1)\ Cs*m*V_b \quad (9)$$

Hence:

$$Cs = \frac{A}{2(E2-E1)*m*Vb} \quad (10)$$

where A is voltammogram area, E2 is input potential, E1 is starting potential, m is mass of active substances and V is scan rate.

Results and discussion

Characterization of cancer cells in the absence of iron ions

Fig. 2 shows CV recorded on the CPE surface in 0.2 M NaCl without (black curve) and with (red curve) tumour cells. Cancer cells led to a remarkable change in CV shape.

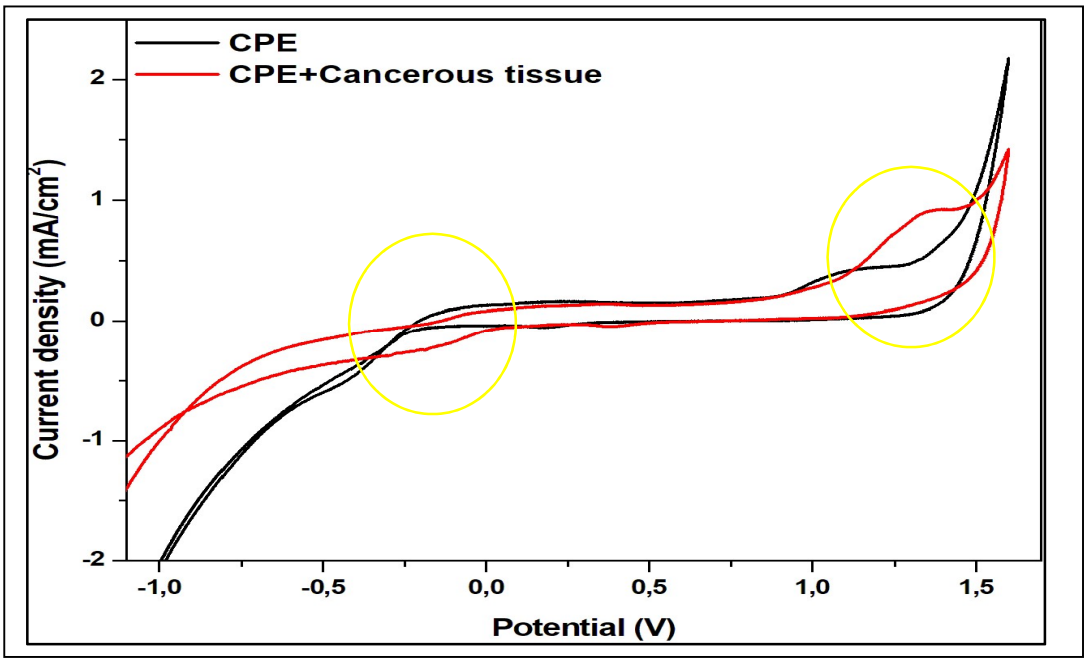

Figure 2: CV recorded at CPE, in 0.2 M NaCl **(a)** without and **(b)** with cancer cells.

This change manifested by the appearance of an oxidation peak at around 1,3 V in anodic sweep direction, due to cancer cells oxidation. The peak at -0,25 V in cathodic scan direction corresponds to cancer cell reduction. Since oxidation and reduction peaks are far apart, one can say that redox process is not electrochemically reversible possibly, due to slow kinetics or unstable intermediates.

Electrons involved in oxidation reactions in cancer cells typically originate from redox-active biomolecules like Reactive Oxygen Species (ROS), Nicotinamide adenine dinucleotide, Flavin adenine dinucleotide or associated enzyme systems.

Fig. 3a-b shows Cs deduced from the area of CV recorded in 0.2 M NaCl without and with cancer cells, respectively. Table 1 shows Cs values for each medium.

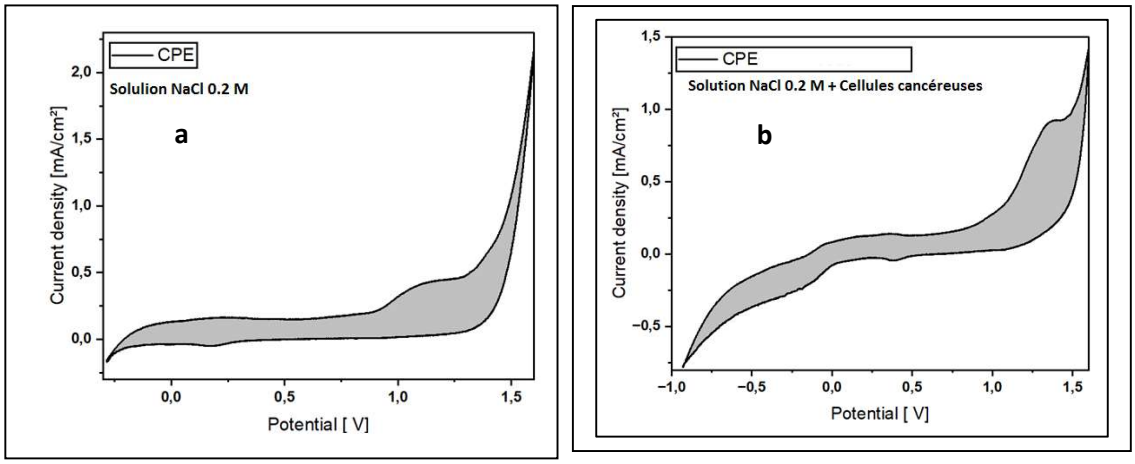

Figure 3: CV recorded at CPE, in 0.2 M NaCl- **(a)** without cancer cells; and **(b)** with cancer cells.

Fig. 3 and Table 1 indicate that Cs after cancer cells addition to the electrolytic medium caused an increase in the capacity to store charge when a potential difference was applied.

Table 1: Difference in Cs between 0.2 M NaCl without and with cancer cells.

Media	Area	Cs
0.2 M NaCl	0.44198776	0.274
0.2 M NaCl with cancer cells	0.6422564	0.911

Fig. 4 presents SWV recorded without and with cancer cells in 0.2 M NaCl.

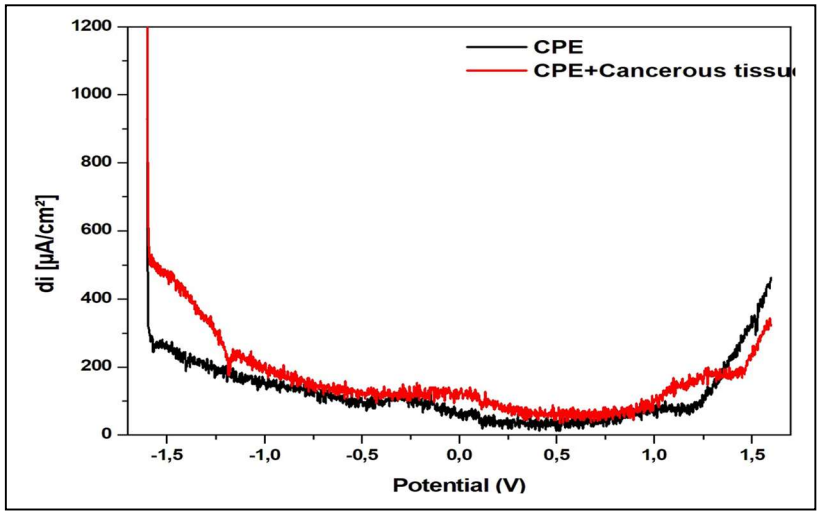

Figure 4: SWV recorded in the surface of CPE with and without cancer cells.

It can be seen that cancer cells in 0.2 M NaCl caused an increase in current densities and the appearance of two redox peaks. The first peak, at around 0 V, is attributed to cancer cell reduction, while the second, at 1.3 V, corresponds to oxidation.
Fig. 5 shows EIS curves recorded at the CPE surface in 0.2 M NaCl with and without cancer cells. These curves have the shape of half-loops of which diameters correspond to CPE resistance to electron exchange with the electrolytic medium. This resistance is much lower when NaCl is enriched with cancer cells. With cancerous tissue, EIS shows two half-loops. At high frequencies, the first half-loops were due to electrons transfer between CPE and cancerous tissue. The second, at low frequencies, correspond to a limited diffusion layer made up of by-products of redox reaction.

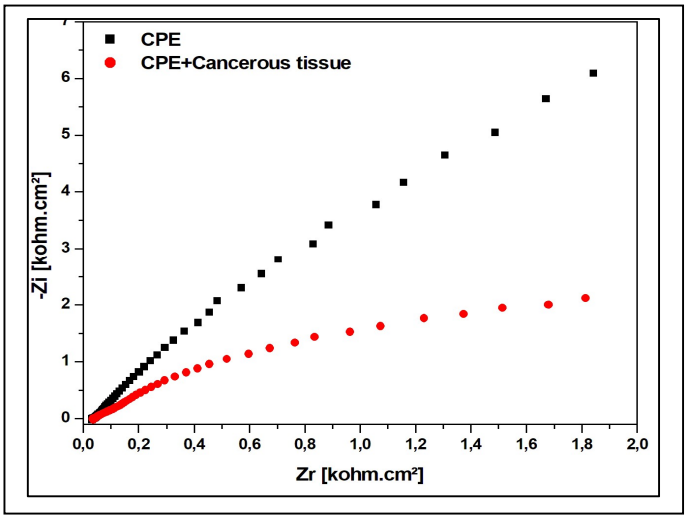

Figure 5: EIS recorded at the surface of CPE with and without cancer cells.

Fig. 6 shows CV recorded in 0.2 M NaCl with cancer cells, at several scan rates. It can be seen that redox peaks current density increased with scan rate.

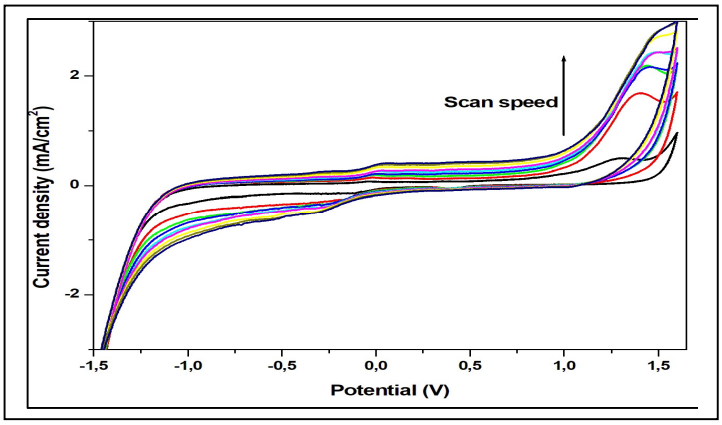

Figure 6: CV recorded at the CPE surface, in 0.2 M NaCl with cancer cells, at different scan rates.

Table 2 presents different Cs vales for various scan rates.

Table 2: Cs registered in different scan rates.

Scan rate (mV/S)	20	40	60	80	100	120	150	180	200
Cs	16	16.9	11.7	10.8	9.3	8.1	7.3	6.5	6.1

Characterization of cancer cells with iron ions

In this study, iron ions were added to NaCl with cancer cells, in order to promote Fenton reaction, and to characterize them. Numerous nanoparticles that react to the tumour's microenvironment have been developed. These agents are stable in normal physiological environments, and undergo chemical modifications when exposed to various conditions present in cancer cells, such as pH, enzymes, reducing conditions and ROS [15-18]. ROS are produced from molecular oxygen (O_2) partial reduction, which is required for normal metabolism of all aerobic organisms. Energy is provided through four electron reduction reactions, and O_2 is converted to water by the following series of reactions (Scheme 1):

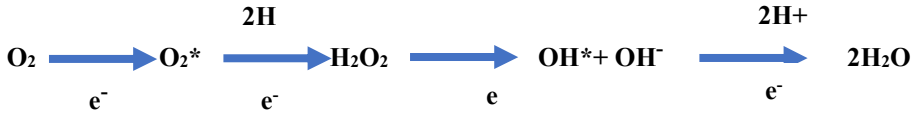

Scheme 1: Series of reactions for ROS.

ROS generation in cancer cells is much alike that with normal ones. Among all ROS, H_2O_2 is generally considered the most abundant and stable non-radical reactive species in cancer cells, and it can be converted to hydroxyl radicals (OH-) in the presence of iron (Fe^{2+}), according to Fenton reaction (Scheme 2) [18]:

Scheme 2: Fenton reaction.

Fig. 7 shows electron transport chain and oxygen reduction processes in living cells.

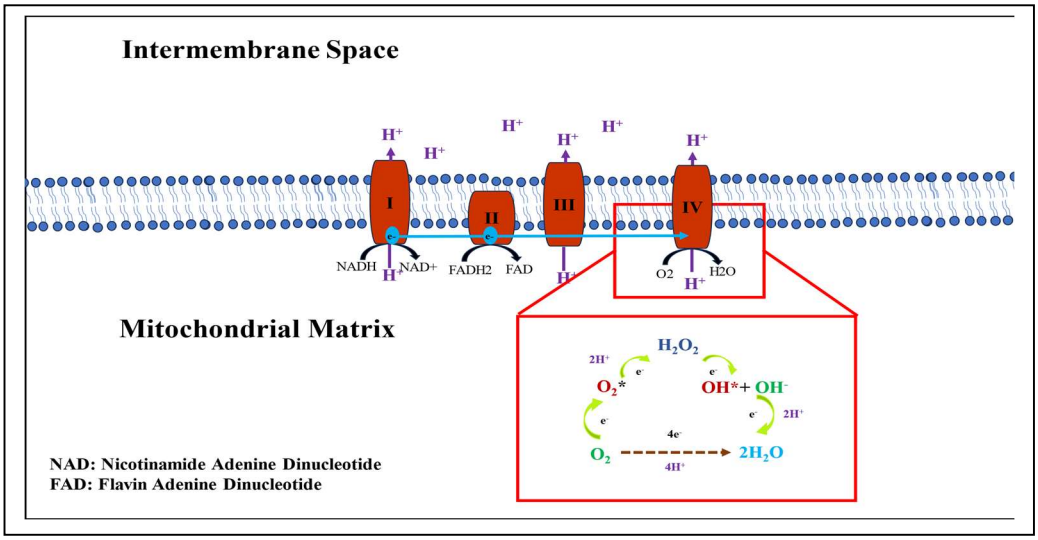

Figure 7: Electron transport chain and oxygen reduction processes in living cells.

Fig. 8 shows CV recorded at the CPE surface in 0.2 M NaCl with Fe^{2+}. The presence of iron ions manifested by the appearance of two redox peaks: the first one in anodic sweep direction, at around 0.8 V; and the second in cathodic sweep direction, at around 0.7 V. This is called a reversible system.

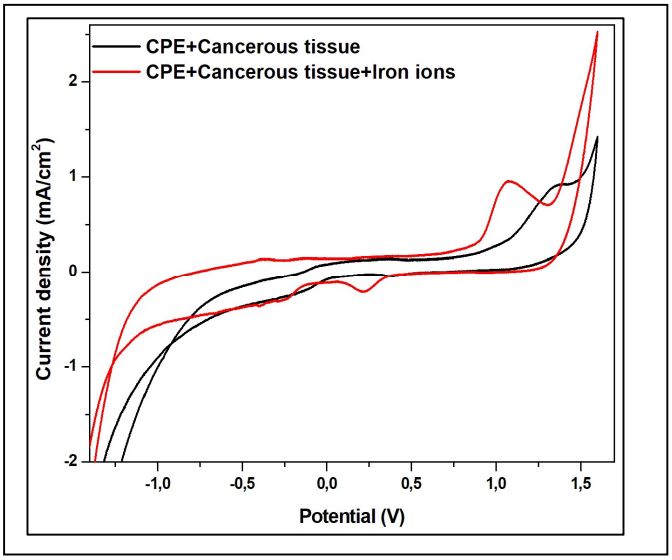

Figure 8: CV recorded at the CPE in 0.2 M NaCl with Fe^{2+}.

Figs. 9-11 show CV recorded at the CPE surface in 0.2 M NaCl with cancer cells without (black curve) and with (red curve) iron ions. With cancer cells in NaCl, the characteristic Fe^{2+} oxidation peak was displaced to 1 V, and reduction peak to 0.3 V, resulting in the system reversibility loss. This displacement in characteristic iron ion peaks was due to interactions between ROS, which are generated by cancer cells, and iron ions in NaCl, according to Fenton reaction.

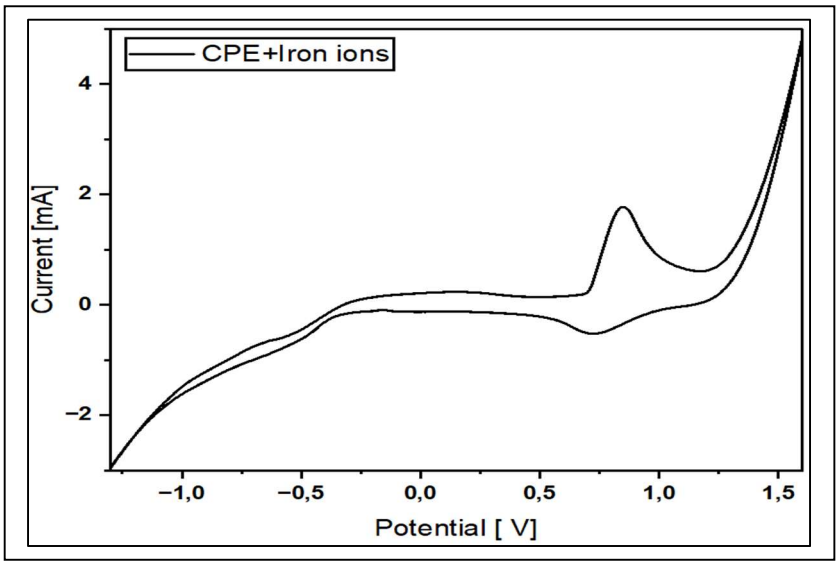

Figure 9: CV recorded at the CPE in 0.2 M NaCl with cancer cells **(a)** in presence and **(b)** absence from Fe^{2+}.

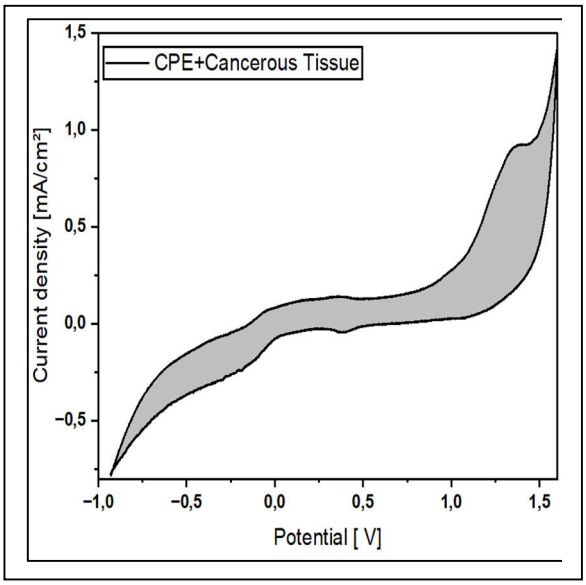

Figure 10: CV recorded at the surface of CPE in NaCl solution with cancer cells.

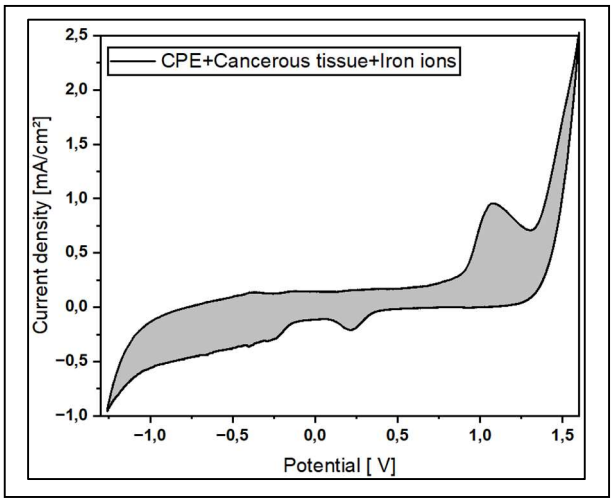

Figure 11: CV recorded at the surface of CPE in a NaCl solution with cancer cells in the presence of Fe^{2+}.

Table 3 shows different Cs values in the presence and absence of Fe^{2+} in an NaCl solution with tumour cells.

Table 3: Cs registered in presence and absence of Fe^{2+} in a NaCl solution with tumour cells.

Media	Area	Cs
CPE + cells	0.6422564	0.911
CPE + cells + Fe	0.19701769	1.011855

Cs was also determined for both CV on NaCl without and with iron ions, to which tumour cells were added. It can be seen that, with Fe^{2+} ions in NaCl, CV surface area increased, leading to a corresponding rise in Cs.

Fig. 12 presents SWV recorded in the absence (black curve) and presence (red curve) of Fe^{2+} in the NaCl solution with cancer cells. It can be seen that Fe^{2+} presence in the electrolyte medium caused the appearance of a peak at around 1 V, which corresponds to the ion oxidation.

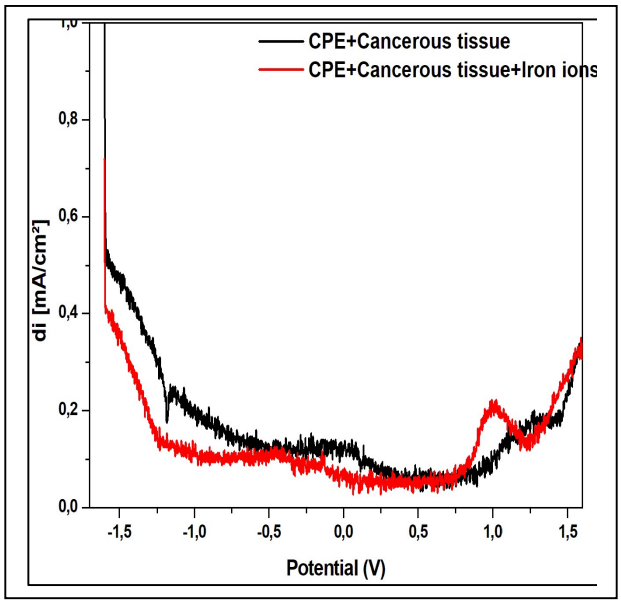

Figure 12: SWV recorded at the CPE surface in NaCl solution in absence and presence of Fe^{2+} ions with cancer cells.

Fig. 13 shows EIS curves recorded at the CPE surface in NaCl with cancer cells in Fe^{2+} absence and presence. These curves are half-loops shape, of which diameters correspond to CPE resistance to electron exchange with NaCl. It can be seen that this resistance is much higher when NaCl contains Fe^{2+}.

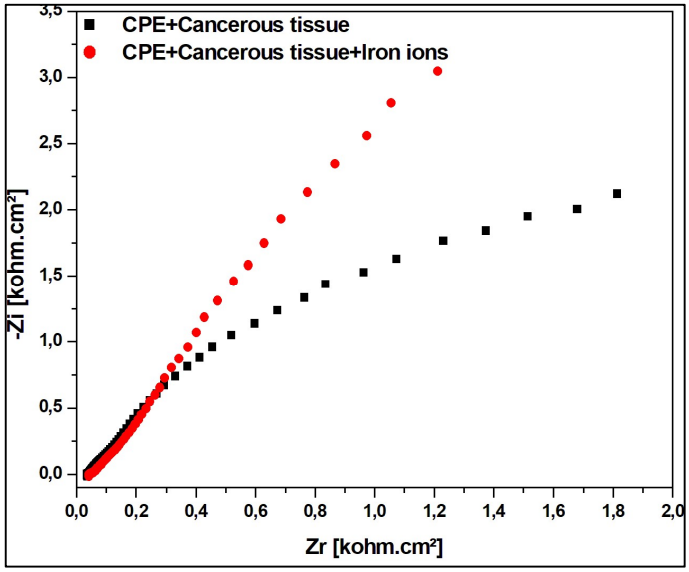

Figure 13: EIS recorded at the CPE surface in NaCl solution in absence and presence of Fe^{2+} with cancer cells.

Fig. 14 shows the effect Fe^{2+} concentration on CV in the NaCl solution with cancer cells. It is clearly seen that, as Fe^{2+} amount increases in the solution, the two characteristic peaks of the ion's redox start to considerably decrease. This decrease is due to the consumption of these ions by the cancer cells present in NaCl.

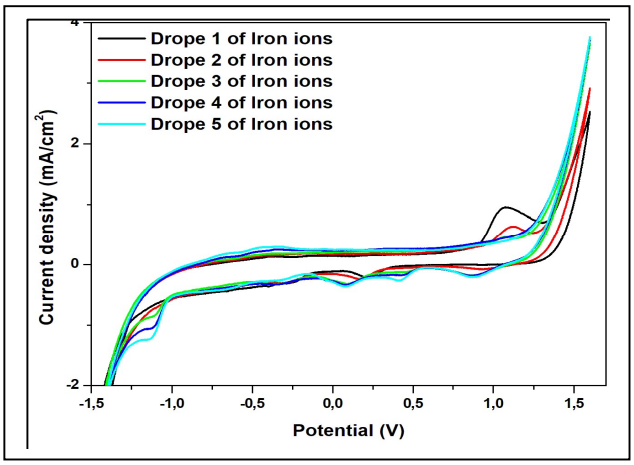

Figure 14: CV recorded at the CPE in the NaCl solution with cancer cells in the presence of different drops of Fe^{2+}.

The effect of scan rate was also studied. Fig. 15 shows CV recorded in 0.2 M NaCl with cancer cells and Fe^{2+} at several scan rates. The increase in current densities with scan rates is explained by the release of the electrode's active sites.

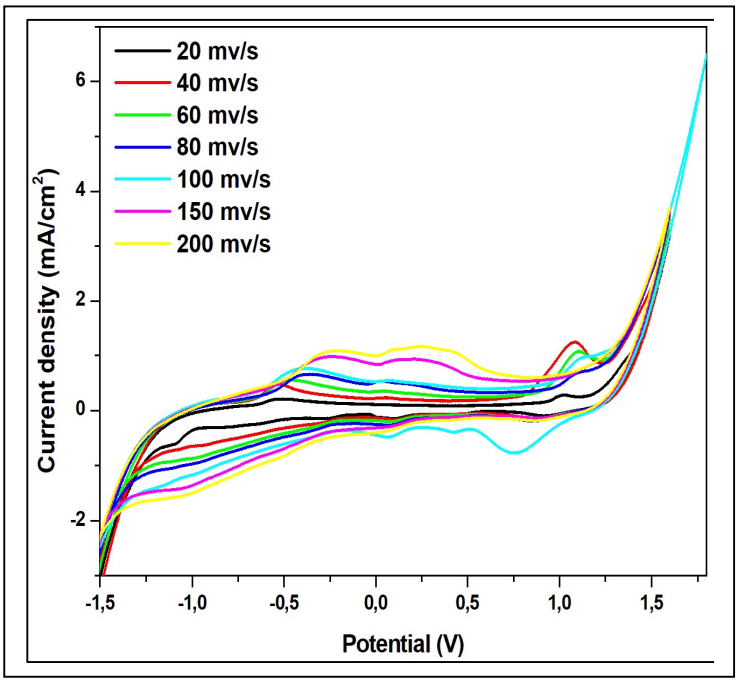

Figure 15: CV recorded at the CPE surface in a NaCl solution with cancer cells at different scan rates.

Conclusion

This electrochemical simplified method holds great promise as a non-invasive and cost-effective solution for follow-up of NMIBC. This approach has the potential to improve patient outcomes, enhance healthcare efficiency and reduce the burden associated with BC management.

Electrochemical biosensors for the characterization and differentiation of cancer tissue have a wide range of industrial applications, such as cancer diagnosis, drug development, tracking in monitoring cancer progression and medical device development.

Authors' contributions

Salma Zahid: corresponding author; did experimental protocol; collected data; wrote original draft. **Hicham El Boté**: contributed to project supervision, experimental investigation and conceptualization. **Abdelilah Chtaini**: supervised the work; validated experimental protocol and final draft.

Abbreviations

BC: bladder cancer
CPE: carbon paste electrode
Cs: specific capacitance
CV: cyclic voltammogram
EIS: electrochemical impedance spectroscopy
NaCl: sodium chloride
NMIBC: non-muscle-invasive bladder cancer
redox: reduction oxidation reaction
ROS: reactive oxygen species
SWV: square wave voltammetry

References

1. Lenis AT, Lec PM, Chamie K et al. Bladder Cancer: A Review. JAMA. 2020;324(19):1980-1991. https://doi.org/10.1001/jama.2020.17598
2. Dobruch J, Oszczudłowski M. Bladder Cancer: Current Challenges and Future Directions. Medicina. 2021;57:749. https://doi.org/10.3390/medicina57080749
3. Jubber I, Ong S, Bukavina L et al. Epidemiology of Bladder Cancer in 2023: A Systematic Review of Risk Factors. Eur Urol. 2023;84(2):176-190. https://doi.org/10.1016/j.eururo.2023.03.029
4. Witjes JA. Follow-up in non-muscle invasive bladder cancer: facts and future. World J Urol. 2021;39(11):4047-4053. https://doi.org/10.1007/s00345-020-03569-2
5. Babjuk M, Burger M, Compérat EM et al. European Association of Urology Guidelines on Non-muscle-invasive Bladder Cancer (TaT1 and Carcinoma in Situ) - 2019 Update. Eur Urol. 2019;76(5):639-657. https://doi.org/10.1016/j.eururo.2019.08.016

6. Witjes JA. Follow-up in non-muscle invasive bladder cancer: facts and future. World J Urol. 2021;39(11):4047-4053. https://doi.org/10.1007/s00345-020-03569-2.
7. von Landenberg N, Benderska-Söder N, Bismarck E et al. Rationale Nachsorge des nicht-muskelinvasiven Harnblasenkarzinoms [Rational follow-up of non-muscle invasive bladder cancer]. Urol A. 2021;60(11):1409-1415. https://doi.org/10.1007/s00120-021-01683-6
8. International Agency for Research on Cancer,
9. Xueji Z, Huangxian J, Wang J. Eds. Electrochemical sensors, biosensors and their biomedical applications. Academic Press, 2011.
10. Doménech-Carbó A, Pontones JL, Doménech-Casasús C et al. Electrochemical detection and screening of bladder cancer recurrence using direct electrochemical analysis of urine: A non-invasive tool for diagnosis. Sens Actuat B: Chem. 2018;265:346-354. https://doi.org/10.1016/j.snb.2018.03.048
11. Zhang Y, Chen S, Sun X et al. Electrochemical biosensors for the non-invasive diagnosis of breast cancer. Electrochim Acta. 2023;468:143190. https://doi.org/10.1016/j.electacta.2023.143190
12. Junpeng L, Jianwen W, Di W et al. Electrochemical aptamer-based biosensing of glycan-conjugated targets. Biom Analy. 2024;1(1):3645. https://doi.org/10.1016/j.bioana.2023.12.003
13. Sanati A, Jalali M, Raeissi K et al. A review on recent advancements in electrochemical biosensing using carbonaceous nanomaterials. Mikrochim Acta. 2019;186(12):773. https://doi.org/10.1007/s00604-019-3854-2
14. Zhao L, Zhou X, Xie F et al. Ferroptosis in cancer and cancer immunotherapy. Cancer Commun. 2022;42:88-116. https://doi.org/10.1002/cac2.12250
15. Akatsuka S, Yamashita Y, Ohara H et al. Fenton Reaction Induced Cancer in Wild Type Rats Recapitulates Genomic Alterations Observed in Human Cancer. PLoS ONE. 2012;7(8):e43403. https://doi.org/10.1371/journal.pone.0043403
16. Ranji-Burachaloo H, Gurr PA, Dunstan DE et al. Cancer Treatment through Nanoparticle-Facilitated Fenton Reaction. ACS Nano. 2018;12:11819-11837. https://doi.org/10.1021/acsnano.8b07635